

**EXPERIMENTAL DETERMINATION OF THE
PARTITIONING BEHAVIOR OF SILVER
BETWEEN VARIOUS SULFIDE PHASES AND
ELECTRUM**

by J. Lynn Youell

Advisors: Professor P.A. Candela and Dr. P.M. Piccoli

Laboratory for Mineral Deposit Research

Geology 394

Fall 2006

Abstract

Silver is always a component of magmatic ore bodies (Robb 2005) at a percentage appreciably greater than gold. However, research in porphyry –type deposits has traditionally focused on the distribution of the more profitable copper, gold and molybdenum constituents. Likewise, epithermal deposits sometimes form in association with porphyry deposits and are an important source of ore because of the higher concentration of precious and base metals typically associated with these deposits. In both porphyry and epithermal type deposits, silver grades are often higher than gold. At Far Southeast-Lepanto, the Ag:Au ratio is approximately 5:1 in grams /tonne (Hedenquist et al. 1998) and 7:1 at the Bingham Canyon porphyry copper deposit. Renewed interest in silver, and the high concentrations found in epithermal deposits inspire research into the distribution of silver especially what constrains the formation of the epithermal ore body.

This study attempts to generate data on the distribution of silver between sulfide phases and electrum that can be used to model and predict factors which can enrich and restrict the formation of a silver-rich epithermal deposit. Since research is lacking as regards the partitioning of silver between sulfide phases and electrum, I have based my research on experimental methods and outcomes in gold distribution conducted by Simon et al. (2000) and experimental determination of the solubility of electrum by Gammons and Williams-Jones (1995) using concentration quotients;

$$K = \frac{x_{\text{sulfide}}^{\text{Ag}} * x_{\text{metal}}^{\text{Cu}}}{x_{\text{sulfide}}^{\text{Cu}} * x_{\text{metal}}^{\text{Ag}}} \quad \text{and} \quad K = \frac{x_{\text{sulfide}}^{\text{Ag}} * x_{\text{metal}}^{\text{Au}}}{x_{\text{sulfide}}^{\text{Au}} * x_{\text{metal}}^{\text{Ag}}}$$

for copper-silver exchange for silver-gold

to connect my research from the data of an actual and a constructed median porphyry deposit, to concentration coefficients developed by Gammons and Williams-Jones (1995) for the exchange of silver and gold and temperature dependencies for exchange reactions. In effect, I am taking my Log K values and interpreting them in the context of the experimental hydrothermal environment (Gammons and Williams-Jones 1995), the paired porphyry copper-gold environment of Far Southeast-Lepanto, and a median porphyry copper deposit described herein. The null hypothesis is: **the partitioning of silver into copper-iron sulfides during the formation of a porphyry copper deposit will be insufficient to poison the formation of a shallow silver-rich epithermal deposit.** I tested the null hypothesis by using my experimental concentration of electrum as the normalizing factor by which I compared the hypothetical concentration of silver and gold in the epithermal ore forming fluid for Far Southeast-Lepanto deposit, a hypothetical median porphyry deposit and an ore fluid derived from Gammons and Williams-Jones research in silver gold exchange. The outcome of these experiments failed to support my null hypothesis.

TABLE OF CONTENTS

Introduction	1
Experimental Method	6
Method of Analysis.....	8
Presentation of Data.....	12
Discussion of Results	16
Conclusions.....	17
Acknowledgements	18
Bibliography.....	19

LIST OF FIGURES

<i>Number</i>	<i>Page</i>
Table 1: Average Abundances of Cu-Ag-Au	1
Figure 1: Porphyry Copper-Epithermal Deposit Model	2
Figure 2: Far Southeast-Lepanto	4
Figure 3: Phase diagram after Simon et al.	5
Photograph 1: Sealed Silica Glass Tubes	7
Photograph 2: Sample of completed Run Products	8
Photograph 3: Finished epoxy section before polishing	9
Photograph 4: Electron Probe Microanalyzer- JEOL 8900	10
Figure 4: EPMA Optical Column	11
Figure 5: Backscatter electron image	11
Table 2: Starting Material	12
Table 3: Electron Results from EPMA	13
Table 4: Copper-iron Sulfides from EPMA	14
Table 5: K and Log K Values for Cu-Ag and Ag-Au	15
Table 6: Summary of Log K Values	16

I. Introduction

In 2005, approximately 1300 metric tons of silver valued at 295 million dollars was mined in the United States. The troy ounce price rose above a seventeen year high set in 2004 to average out at eight dollars an ounce. Silver is expected to hit a new high this year as well. According to the U.S. Geological Survey's mineral commodities summary (2005), the deficit between the supply and demand for silver was approximately 1700 metric tons world wide.

Silver has traditionally been an inexpensive alternative to gold for jewelry, tableware and coins. With a surge in digital photography, silver's stronghold as a film coating has dwindled; however, its use in micro-technology, electronics, industry, and medicine, combined with its low cost, have made it increasingly appealing to investors. Most silver is mined as a secondary product or recycled from scrap. The majority of the world's silver supply is associated with copper, zinc and lead deposits as a by-product of ore processing. Of particular interest are magmatic hydrothermal deposits known as porphyry copper deposits which are the primary sources for copper, gold and molybdenite. Distal to the porphyry copper deposits, epithermal silver ore deposits can occur. Epithermal deposits are an important source of ore because of the higher concentration of precious and base metals. However, associated silver-rich epithermal deposits may not form in some cases (Candela, personal communication, 2004). Recoverable silver, either as a constituent of the porphyry copper deposits or as an epithermal deposit is not guaranteed, although silver is always a component of magmatic ore bodies (Robb 2005) at a percentage appreciably greater than gold (Table 1). Was the magmatic source of the ore constituents silver poor or was the silver trapped in the deeper sulfide phases of the porphyry copper deposit? That is; is the formation of a silver-rich epithermal deposit poisoned by the formation of the porphyry copper deposit? Because research in porphyry -type deposits has traditionally focused on the distribution of the more profitable copper, gold and molybdenum constituents, little is known about the distribution of silver. I proposed a series of experiments to test the distribution of silver in the sulfide phases commonly associated with porphyry copper deposits. My null hypothesis is; **the partitioning of silver into copper-iron sulfides during the formation of a porphyry copper deposit will be insufficient to poison the formation of a shallow epithermal deposit.**

Average Abundance of Cu, Ag and Au in Major Magma Types find a number to fill in for Au.

	Basalt	Andesite	Rhyolite
Cu (ppm)	65	60	6
Ag (ppb)	100	80	37
Au (ppb)	3.6	----*	1.5

Table 1 adapted from Robb (2005) *No data is available for Andesites reservoir and gold concentration according to Geochemical Earth Reference Model (earthref.org 2006)

Porphyry copper deposits are associated with shallow, intermediate to felsic magmatic intrusions in arc environments. According to the magmatic-hydrothermal theory (Candela, 1992) for the formation of a porphyry copper deposit, magma moves upward into the Earth's crust. Magma is a mixture of melt \pm crystals \pm bubbles and is less dense than a mixture of solid phases of the same bulk composition at the same pressure. The hydrous magma body becomes emplaced in the upper levels of the crust, generally the upper twelve kilometers, when the magma degasses and crystallizes. Cooling begins on the outer margins of the magma body in contact with the cooler country rock.

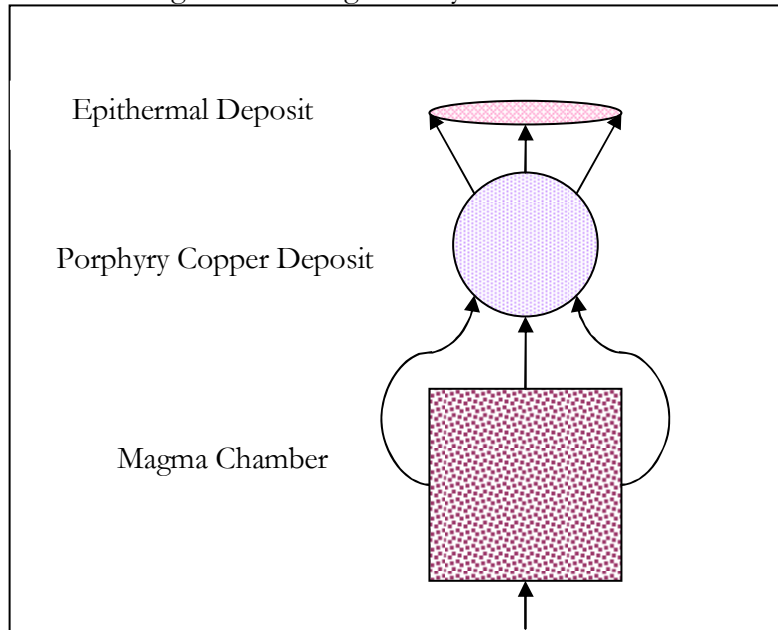


Fig 1: Simplified schematic of a paired porphyry/epithermal deposit. Arrows indicate the general path of fluid flow.

The mineral deposit(s) are the result of the hydrothermal solutions that become superheated vapors that move through the surrounding country rock along existing veins or by fracturing the host rock and creating new pathways. The solutions are rich in dissolved solids including base and precious metals and containing anywhere from 1-50% solids by weight (Skinner 1997).

In the laboratory, plagioclase crystallization begins at 1100° C, at 200 MPa pressure and water concentrations of a few weight percent. Under these conditions, the last silicate melt disappears at approximately 680° C, so there is a 400° C crystallization interval. As the melt crystallizes, bubbles (vapor) form. This occurs for two reasons:

1. Response to the lowering pressure as the magma body rises.
2. Crystallization of anhydrous minerals. (Candela 1992).

Decreasing pressure and crystallization allows water and other volatile constituents to increase in concentration. Once the melt is saturated with respect to the volatile phase, H₂O, CO₂, HCl, H₂S, and SO₂ bubbles form. This volatile phase contains dissolved solutes: NaCl, KCl, FeCl₂, SiO₂, CuCl, H₂AuCl₂, and AgCl, etc. Volatile phase exsolution is accompanied by an increase in volume and the increased fluid pressure results in the generation of a network of fractures around the magma body. Once fractured, the magma body can decompress further, and the quenched magmatic volatile phase

can interact with the country rock leading to mineral deposition. Most commonly the copper iron sulfide minerals, chalcopyrite (CuFeS_2), pyrite (FeS_2), and bornite (Cu_5FeS_4) dominate (Ballantyne 1997). This interaction “roofs” the magma chamber and forms a cupola as part of the intrusion akin to a bump on the top of the chamber. It is above this structure that sulfide mineralization occurs; altering the country rock into the region known as a porphyry copper deposit typically enriched in gold, molybdenite, lead, zinc and sometimes silver.

Epithermal deposits are seated at shallow depths of approximately one or two kilometers and are the products of the volcanic hydrothermal activity that produced the porphyry copper deposit (Sillitoe and Bonham 1984). Epithermal deposits are not as well understood. Magmatic waters continue to rise above the porphyry copper deposit and with a continuing drop in temperature deposition of base and precious metals occurs. Epithermal deposits are formed at shallow depths and as such, the potential exists for a mixing of meteoric and magmatic waters, metamorphic waters driven out by dehydration as well as the addition of ground water to further complicate the formation of a deposit (Skinner 1997). Water enriched in silver and gold ions will flow more readily through areas of less dense host rocks in response to the heat of the igneous intrusion, thereby concentrating the metals. The conditions necessary for the formation of the epithermal silver deposits above the cupola of a porphyry copper deposit are the higher temperature (+ 1000° C) and drier magmas associated with arc related, Andean - type subduction zones (Robb 2005).

An excellent example of a paired porphyry copper and epithermal deposit is the Far Southeast-Lepanto (FSE-L) porphyry and epithermal copper- gold deposit in Luzon, Philippines (Figure 1, below). Temperature estimates for FSE-L based on fluid inclusions give early alteration and homogenization temperatures of 450°-550°C with a decrease of temperature with increasing distance from the ore body (FSE) to 295°-200°C. The porphyry copper deposit known as Far Southeast has a cutoff grade of 1. % Cu equivalent, and 2.5 times that for the Lepanto epithermal body (Hedenquist et al. 1998). One-quarter of the copper and gold available at FSE-L is contained in the smaller and more accessible Lepanto epithermal body. This alone explains the importance of epithermal deposits.

Lepanto is also mined for silver, with 1992 production totaling 10.7 g/tonne or approximately 100 tonnes of silver. This is approximately 5 times the amount of gold mined from Lepanto, but silver’s lower value makes it worthy only of mention. This economic bias points out the difference between the geochemical importance of a metal and the value assigned by the needs of society. Such is the fate of other ores in history. For instance, at the turn of the last century, sandstone vanadium-uranium deposits were mined extensively for the rare element vanadium and the uranium was discarded as part of the mine tailings. With the development of atomic weapons and later, nuclear power plants, the sandstone deposits became known as uranium mines. Even though they contained more vanadium than uranium, and had originally been mined for vanadium, the demand for uranium changed how the mines were represented. With renewed interest in vanadium in the 1990’s, the mines became uranium-vanadium deposits (Candela 2004). This example highlights the care that must be taken to separate the economic from the geochemical.

Far Southeast-Lepanto Copper-Gold Porphyry and Epithermal Deposit

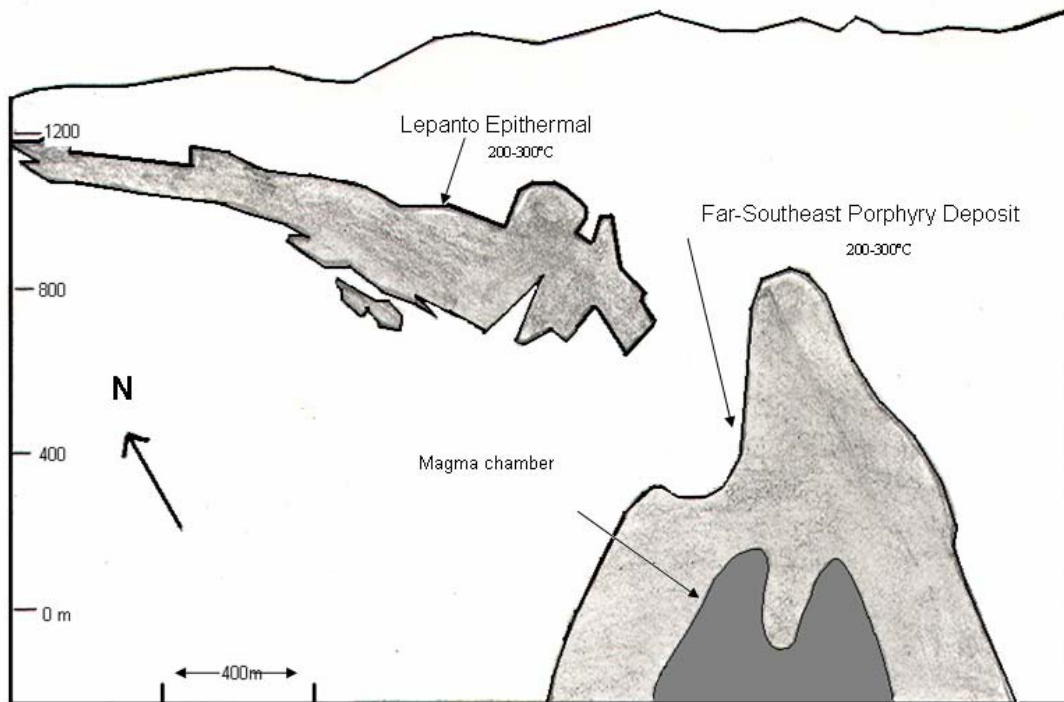


Figure 2: Adapted from Hedenquist et al. 1998

Previous work by Solomon (1990), Candela (1992), Hedenquist and Arribas (1998), Ulrich, et al. (1999), Simon, et al. (2000), Halter, et al. (2002), and Heinrich, et al. (2004), focused on the genesis of porphyry copper deposits and the ore metal ratios of copper, molybdenum and gold. Since silver can be expected to occur in similar settings and under similar conditions as gold (Robb 2005 and Table 1), the research involving gold can be illuminating and relevant to understanding the deposition of silver ore deposits that have a magmatic origin.

Solomon's (1990) work suggests that island arc porphyry copper- gold deposits are dependent upon arc reversal during formation in order to host the ore rich sulfide deposits. Similarly, Hedenquist and Arribas (1998) examined the same type of copper- gold porphyry copper deposit as Solomon (1990) but examined the spatial association of two porphyry copper deposit deposits: the Far Southeast - Lepanto and the Guinaoang Porphyries, and the development of epithermal gold deposit at one and not the other.

Candela (1992) points out that the amount of metal available to form deposits can be limited if the magmatic volatile phase exsolution occurs late in the crystallization of minerals from the melt,

limiting or precluding the formation of an ore deposit by sequestering the metals in the minerals. Similarly, Heinrich, et al. ((2004) interpreted a physical and chemical link between hydrothermal vapor/fluid evolution and the deposition of gold in porphyry copper deposits using thermodynamic and fluid inclusion data. Ulrich, Gunther and Heinrich (1999), showed that the concentration of Cu-Au in porphyry copper deposits is a function of the ratio of the metals in the high temperature brine, and consequently, a function of the crystallization of the magma.

Experimental distribution of gold in the Cu-Fe-S system at 600°C by Simon, et al. (2000) demonstrated an affinity by gold for bornite. Experiments in the Cu-Fe-S system at 400-700° C used gold powder, stoichiometric bornite powder and chalcopyrite to determine how much gold could be accommodated in bornite. The experiments demonstrated that gold concentrations in bornite:

1. Decreased with a decrease in temperature.
2. Decreased in both Cu- rich and Cu- poor end members of bornite
3. Increased in both stoichiometric and intermediate solid solutions at temperatures of 600-700°C relative to lower temperature experiments.
4. When saturated with respect to gold, bornite can accommodate 1 weight percent of gold- but it is present as masses at the boundaries of bornite grains and can be lost or redistributed at temperatures of 700°C or greater.

Their experiments also indicated that a significant amount of gold can be lost into the surrounding hydrothermal system. Equilibrium was not achieved in the 600-700°C experiments as demonstrated by the variation of gold in the intermediate solid solution and bornite. Gold and silver, both members of the 1B transitional elements can be hypothesized to behave in a similar manner; consequently, this paper presents a model for the possible evolution of an epithermal silver deposit as well and the investigation by Simon et al. (2000) offers the framework for an investigation of silver distribution in sulfide phases, as well as a model for dry sulfide research.

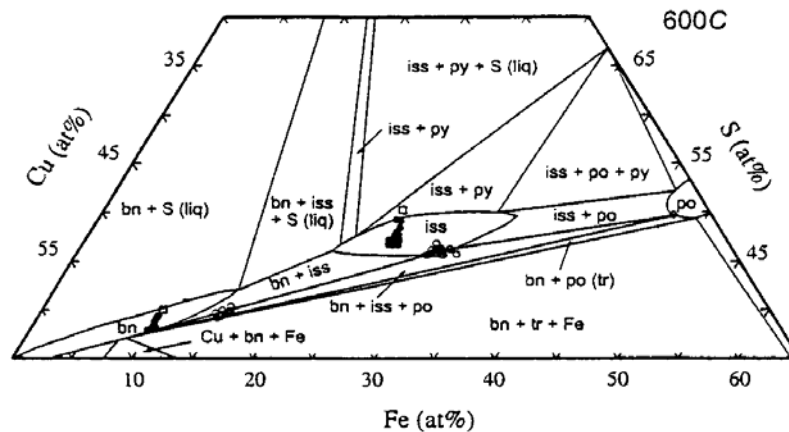


Figure 3: Adapted from Simon et al. (2000) Black circles represent compositions in equilibrium with gold in research by Simon et al. Open circles represent their gold-bornite-pyrrothite assemblages. Open squares are stoichiometric bornite and chalcopyrite compositions.

To better understand porphyry copper deposits and epithermal deposits, I examined data on a median porphyry copper /epithermal deposit I'll call the Median Porphyry Copper Deposit of North America. To elucidate my model, I will describe a hypothetical median porphyry copper and its associated median epithermal deposit of copper, silver and gold which occur in both the porphyry

copper and epithermal deposit. The porphyry deposit will be 10 km^3 so based on a weight of 3000 kg/m^3 yields approximately 3×10^7 tonnes of magma. The ore metals will be derived from an andesitic magma with concentrations of Cu ~ 60 ppm and Ag is 60 ppb well within established limits (Robb 2005 and Table 1, p. 2) and the ratio of Cu/Ag is 10^3 . Fifty percent, a reasonable “efficiency of removal” of the metals from the parent magma will be available to the ore forming aqueous fluid (Candela and Piccoli 1995). So 30 g of copper /tonne will “get out” of the magma, yielding 10^6 tonnes of copper. Silver concentration at fifty percent efficiency will be 30 ppb or 3 magnitudes less than copper or $\sim 10^3$. Since gold abundance in andesite is unknown, I will use the figures from Far Southeast-Lepanto (2 g/ t of ore) as a reasonable estimate for the median magma, and this will yield 2×10^2 tonnes of gold from the magma. Consequently, the median porphyry copper deposit has 10^8 tonnes of copper, and 10^2 tonnes of silver and 10^2 tonnes gold.

Of particular interest is the epithermal deposit which will yield 10^7 tonnes of ore and one-quarter the tonnage of silver as Lepanto at a concentration of 10g/ tonne (Hedenquist et al. 1998) consistent with the median deposit being one-quarter the size of Far Southeast- Lepanto. This will yield 10^2 tonnes of silver in the median epithermal deposit. This is approximately ten percent of the silver available from the parent magma. If something prohibits the delivery of 10% of the magma to the epithermal deposit, no deposit will form. It is the goal of my project to examine some of the sulfide phases in the porphyry copper deposit as factors that can poison the evolution of an epithermal deposit.

Ballantyne (1997) indicates that silver is inferred to be present in solid solution with sulfide minerals associated with porphyry copper deposits. Copper- iron sulfides are the primary ore minerals in porphyry copper deposits. Likewise, chalcopyrite and bornite are host sulfides for gold particles (Ballantyne 1997), and Simon, et al. (2000) indicate that “stoichiometric” bornite can accommodate 1280 to 8200 ppm gold in laboratory experiments. Silver, a member of group IB, also occurs naturally with bornite, and the research on the partitioning of Ag between gold (electrum) and bornite can be utilized to investigate the behavior of silver in the sulfide phases of porphyry copper deposits. Based on the research by Simon, et al., I proposed a series of similar experiments in an effort to determine the partitioning behavior of silver and an equilibrium constant, K, for the controlling equilibrium. Since gold has a high affinity for silver, forming the alloy electrum (Robb 2005), the experiment included gold metal in an effort to generate a realistic appraisal of the partitioning behavior. I tested the null hypothesis that: the partitioning of silver into copper-iron sulfides during porphyry copper deposit formation will be insufficient to poison the formation of a more distal epithermal deposit. Therefore, the partitioning of Ag into Cu-Fe sulfides will be insufficient to poison the formation of a more distal epithermal deposit. Thus the experiments provide data that will contribute to increased profitability of silver mining in conjunction with porphyry copper deposits. My study will attempt to determine an apparent equilibrium constant for the exchange of copper, silver and gold between electrum and copper-iron sulfides of variable composition. My apparent equilibrium constant- K is written in terms of concentration, not activities so that K can vary as a function of the concentrations included in the expression:

$$K = \frac{x_{\text{sulfide}}^{\text{Ag}} * x_{\text{metal}}^{\text{Cu}}}{x_{\text{sulfide}}^{\text{Cu}} * x_{\text{metal}}^{\text{Ag}}}$$

for copper-silver exchange

(Each x value is the mole fraction for the silver, copper or gold in the electrum (metal) phase or the sulfide phase.)

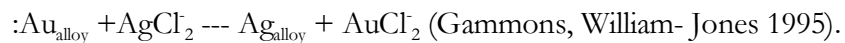
and

$$K = \frac{x_{\text{sulfide}}^{\text{Ag}} * x_{\text{metal}}^{\text{Au}}}{x_{\text{sulfide}}^{\text{Au}} * x_{\text{metal}}^{\text{Ag}}}$$

for silver-gold.

These apparent equilibrium constants allow me to estimate the ratio of the concentration of the metallic silver to both copper and gold in a copper iron sulfide gold and silver bearing system at 600°C. This can be equated to dipping a piece of electrum into the mobile hydrothermal fluid during the formation of the porphyry copper deposit and then analyzing the concentrations of silver, copper and gold to determine the resulting equilibrium ratios of the metals. This, in turn, yields an estimate of the concentration ratios of the metals in the ore-forming environment.

A geochemical model for the solubility of electrum (Au-Ag) alloy and chlorargyrite in brines at 300°C was examined by Gammons and Williams-Jones (1995). The resulting data provide a foundation for transforming my equilibrium constants (expressed as log K values) from dry sulfide-alloy systems into a form that can be used for relating sulfide minerals in aqueous solution to actual porphyry copper deposits. Gammons and Williams-Jones measured the solubility of electrum in brines at 300°C to determine the partitioning of Au and Ag between electrum and a chloride bearing aqueous solution expressed in their reaction 19 as:



The values obtained show that silver is five orders of magnitude more soluble than gold and as such the authors derived from experimentation that for one grain of electrum the solution must contain approximately 100,000 times the silver as gold (Gammons, Williams-Jones 1995).. Temperature dependency for the silver – gold reaction expressed by reaction 19 can also be demonstrated by the regression equation derived for log K versus 1000/T, in Kelvin, which gives me a means to extrapolate the Au-Ag exchange in my dry experiments to the wet conditions of a hydrothermal system.. Equation 1: **y (log K) = 0.73971- 3.6097x (1000/temperature of experiment in K) (no relative error given)** will be used to calculate a corresponding log K value for the temperature of my experiments.

My experiments were conducted at 600°C or 873 K. Based on the Arrhenius relation above I can make an order of magnitude estimate of my log K for Au-Ag exchange in the hydrothermal environment. When T = 873 K, x = 1.15, and log K is approximately -3. Changes in pressure had minimal effect on the outcome (Gammons, Williams-Jones 1995), (Barton, P. 1964).

II. Experimental Method

I used the dry sulfide techniques developed by Kullerud (1971) and used by Simon, et al. (2000), to study the partitioning of silver between sulfide phases, silver and gold foil. According to Kullerud (1971), dry sulfide synthetic experiments can be run in high-purity silica glass tubing. For my experiments, I sealed one end of the silica glass tubes by heating over a methane- oxygen flame, then rinsed the tubing with acetone to minimize static electricity and loaded each tube with a sulfide phase, acanthite or silver, and gold. Initially, the tubes contained 15 mg. finely ground ~2 microns of various sulfide phases from the laboratory general collection, 10 mg. gold metal and 1-5 mg. of silver foil,

weighed on a Mettler 240 electronic balance (% error $\pm .00005$ (1σ)) as determined by the repeated weighing of a standard balance weight where one standard deviation equals:

$$\sigma = \sqrt{\frac{\sum (x - \bar{x})^2}{n - 1}}$$

Subsequent experiments contained 15 mg sulfide phase 10 mg gold foil and 4 mg silver foil or 10 mg acanthite.

First, the starting materials were prepared for use. The sulfide phases were ground and picked through for gross impurities like pyrite and quartz, then re-examined under 50x magnification binocular microscope with a fiber optic light source and picked again. The gold metal was cleaned in a weak HCl bath, placed in a 120° C oven for one hour while new silver foil was examined and cut to ~1 mg squares. The starting materials were weighed, recorded and placed in individual silica glass tubes then placed in a 120°C oven to remove any moisture from handling. Once filled and dried the prepared tubes were sealed then weighed and assigned a number. Tubes were numbered sequentially and numbers were not reused in the event of a failed run.



Photo 1. Sealed silica glass tubes

Since the tubes were not filled completely with the starting materials and silica glass is a rigid material, vapor, in the form of sulfide gas, will be an inherent part of the experiment. To minimize vapor pressure as well as eliminate O₂, CO₂, N₂ and H₂O, the tubes were evacuated by a vacuum pump during sealing. The small amount of gaseous sulfur produced should not be sufficient to adversely affect the experiment (Candela, personal communication, 2004). After sealing, the tubes were weighed, the bulk weights recorded, and the tubes numbered. The filled tubes were then placed in a furnace calibrated to 600° C \pm 5° C by using a chromel-alumel thermocouple as recommended by Kullerud (1971) and heated for a period of 7 to 56 days. After the specified period of time, the loaded tubes were removed from the furnace and rapidly quenched to room temperature by immersion in a cold water bath.

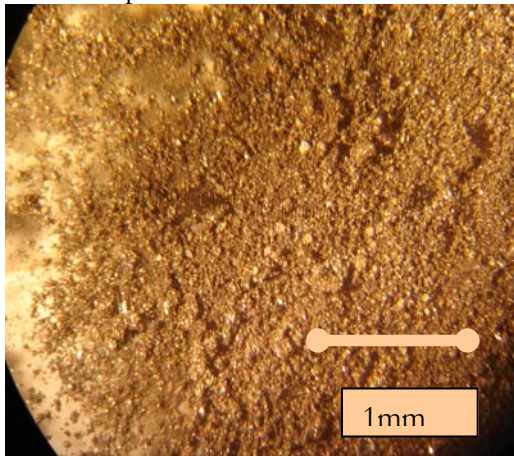
Finally, time invariance was the method selected to determine equilibrium. Three outcomes are possible for time invariance:

- Un-reactivity- no change in the starting materials
- Steady State- a continuous input and output of material, i.e., an open system.

- Time invariance- equilibrium has been achieved if different experimental run times scatter around or approach an average value.

The data demonstrate that there was a change in the starting material since the final phases differed from the starting phases, so un-reactivity is rejected. The experimental setup is closed, so steady state is also removed from the list of outcomes. Therefore, time invariance remained the only possibility for equilibrium in my experiments (Jugo, et al. 1999).

Experiments one through eight varied the ratio of starting materials: sulfide: silver: gold to determine an optimum ratio for reaction. Based on feedback from those experiments, the next eight experiments (9-16) held the ratios of materials constant and varied the time (7-56 days) in an effort to establish equilibrium. Finally, experiments seventeen through twenty two were conducted using silver as acanthite powder instead of silver foil due to the inconsistent assimilation observed in the first sixteen experiments.



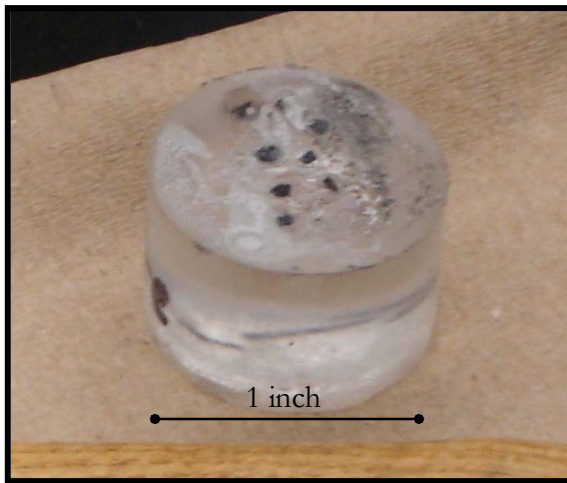
Photograph 2: Sample of completed products

III. Method of Analysis

Once quenched, the tubes were re-weighed and matched to their original number. This step eliminated any failed runs identifiable by weight loss or gain due to water seeping into the tube. The tubes were opened and the products observed under a microscope at 50x magnification reflected light microscopy. Well-formed crystal structures and gold metal were the desired products for analysis. For analysis, the gold metal was secured to the edge of a petrography slide and then set aside. The sulfide products selected from the run were mounted on double-sided tape secured to the bottom of the plastic form. The cylindrical form is fitted to the bottom, and the petrography slide with the gold metal is placed on edge beside, but not touching, the other run products. The clear epoxy was mixed, 15 parts resin: 2 parts hardener with a small stirrer, slowly incorporating the two parts together with out the introduction of air bubbles. Once mixed, a clear homogeneous mixture resulted. The mixture was then slowly poured into the molds to approximately half full. After 30 minutes a small typed label with the run number and my initials was placed on the poured epoxy, and a second batch was mixed following the same procedure to fill the remainder of the mold.

The epoxy was allowed to harden approximately 48 hours; until it was dry and hard to the touch. The epoxy form was removed by gently tapping the mold to release. The section was

examined for integrity; firmly embedded products, and a solid resin that was not sticky, cloudy, or bubbly. The rough sections required polishing to a smooth, nearly scratch free surface. The first polish was done using 330 grit silicon-carbon (SiC) sandpaper on a rotary sander, and then hand polished in five phases beginning with 15-micron diamond paste and Beuhler polishing oil, through successively finer grades of 9, 6, 3, and 1 micron diamond paste.



Photograph 3: Finished epoxy section before polishing

After each phase of polishing, the sections were be washed thoroughly in soapy water, rinsed in clear water and alcohol, and dried. The hand polishing was done first in one direction and then perpendicular to that direction for the next polishing level. To accomplish this right angle polishing an arrow was drawn on the top of the section with an indelible pen or the petrography slide's edge was used as a directional marker. It is important to examine the section under the reflected light microscope between each polishing to assure a smooth surface. Once polished, the sections were coated with carbon for electron probe microanalysis (Piccoli, personal communication, Oct. 2004). This step in the research process was guided by Dr. Philip Piccoli and conducted in the microprobe lab.



Photograph 4: Electron Probe Microanalyzer- JEOL 8900

Electron probe microanalysis (EPMA) is the diagnostic information produced by the electron microscope. It was designed to analyze and image solid materials. Electrons are produced by a hot filament near the top of the column (see figure 2) which are then accelerated down an evacuated column, and focused and filtered through a variety of lenses and apertures to finely focus on a specimen (Donovan 1992). The specimen is thereby bombarded with electrons, and, because electron bombardment of matter produces X-rays, X-rays are generated, with the wavelength characteristic of a given element, and the intensity of the radiation proportional to the concentration of the element in the specimen. The resulting x-rays are “read” by an x-ray detector and the data collected can be read as energy dispersed spectroscopy (EDS) or wavelength-dispersed spectroscopy (WDS). EDS is used to determine the elements present and their relative abundance (qualitative). The WDS is used for quantitative chemical analysis. The starting bornite was analyzed using EDS to confirm its chemical composition, whereas the polished sections are analyzed using the more rigorous WDS to determine the concentrations of elements present (Donovan 1992). The electron microprobe is capable of spatial resolutions of $\sim 1\mu\text{m}$, analytical sensitivity $<0.5\%$ for major elements and detection limits of $\sim 100\text{ppm}$ for trace elements (Donovan 1992). Functionally, the percent error is $300/30000$ or 1% (Piccoli, personal communication, Oct. 2004).

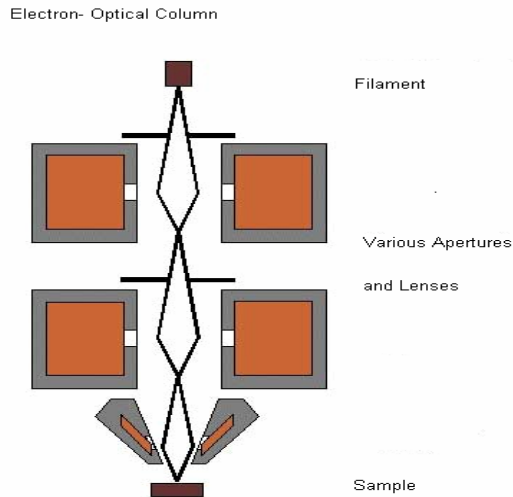


Figure 4 Electron Microprobe optical column: Adapted from University of Oregon EPMA handout

EDS and WDS were used to analyze phases in individual crystals and the gold metal. Phases appeared in gray scale on the CRT monitor as backscatter electron images used to view the specimens in the EPMA.

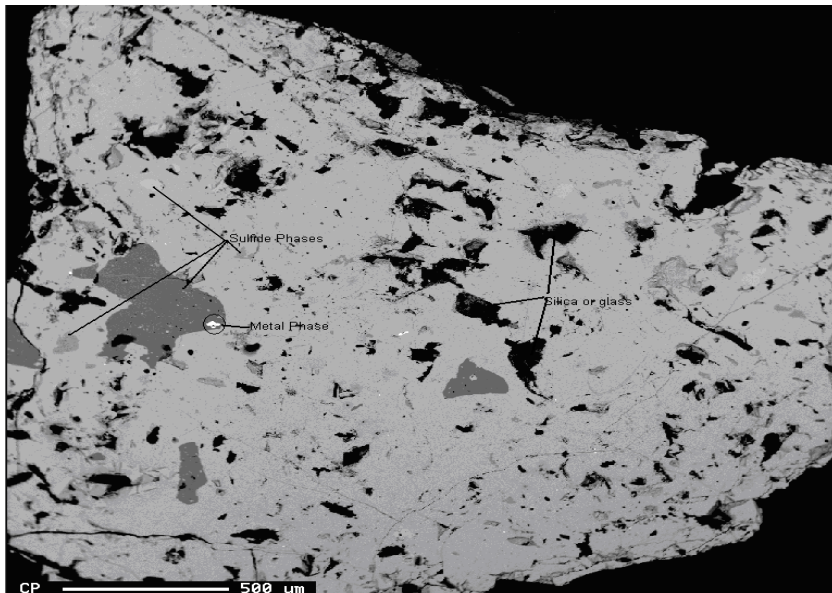


Figure 5: Backscatter- electron image

Backscatter electron imaging was used to identify phases and as a reference guide for WDS. Different phases appeared as different shades with distinct boundaries separating each. The bright white represents a metal phase (Au, Ag, etc.), various grays represent sulfide phases, black is glass or quartz.

IV. Presentation of Data:

From the twenty two experiments conducted, data are included for the successful runs (17, 19-22) identified by the presence of both a copper-sulfide and electrum phase and no significant weight loss. In some experiments, success was determined by the complete adsorption of silver foil into the copper-iron sulfide and electrum phases. This chart shows the concentration of the starting products for the runs analyzed by WDS. Run 18 is not included because there was no change in the starting material, i.e., no silver in the gold foil, and/ or no gold, silver in the copper – iron sulfide phases.

Table 2

Phases (in milligrams) of Starting Material
Sulfide Phases

Sample #	Bornite	Chalcopyrite	Gold	Acanthite
17	15.01	1.0	4.07	10.35
19	15.02	1.0	4.05	10.02
20	14.99	1.0	4.00	10.03
21	14.98	1.2	4.01	10.03
22	15.10	1.2	4.01	9.98

(Weighed on Mettler AE 240 ± 0.0005 grams)

The resulting run products from WDS for the successful runs are presented in atom percent for both the electrum and copper-sulfide phases

Table 3

Analysis of Electrum in Runs 17-22 for Atom % of Elements **

Electrum	Element in		Atom %			Total Atom %
Sample #	Ag	S	Au	Cu	Fe	
Run 17:	0.0724	0.2753	97.7677	1.8846	0	100
	0.0945	0.4975	97.9015	1.4666	0.04	100
	0.082	0.0179	98.9686	0.9314	0	100
	0.0698	1706	98.8615	0.8981	0	100
Run 19:	0.0372	0.1559	98.805	0.9463	0.0556	100
	0.0268	0.3605	98.6391	0.9735	0	100
	0.1129	0.1648	98.2056	1.5167	0	100
	0.0677	0.1542	98.5109	1.2671	0	100
	0.1148	0.3354	98.1854	1.3354	0.0289	100
	0.0873	0.3048	98.3776	1.2304	0	100
Run 20:	0.0087	0.1009	98.6582	1.1869	0.0454	100
	0.0477	0.1761	98.2884	1.4878	0	100
	0.0651	0.117	98.5194	1.2957	0.0028	100
	0.0356	0.1068	98.6799	1.1777	0	100
	0.0387	0.136	98.5669	1.2583	0	100
	0.0718	0.0098	98.4789	1.4395	0	100
Run 21:	0.1544	0.1016	98.2485	1.4322	0.0634	100
	0.1076	0.0257	98.7668	1.0687	0.0312	100
	0.0717	0.073	98.9229	0.9324	0	100
	0.0574	0.2794	98.7506	0.9126	0	100
	0.0267	0.0113	99.1313	0.8001	0.0306	100
	0.0284	0.1644	98.9988	0.7947	0.0138	100
Run 22:	0.2245	0.1365	97.9087	1.7304	0	100
	0.1913	0.1767	98.0272	1.6048	0	100
	0.2179	0.2668	97.8195	1.6958	0	100
	0.2454	0.3682	97.5271	1.8593	0	100
	0.1787	0.1363	98.1246	1.4725	0.0878	100
	0.142	0.0893	98.5262	1.2425	0	100
	0.1825	0.0781	98.311	1.4217	0.0067	100

* Run #18 not included, see discussion.

± 1 % (1σ) –see discussion of microprobe

Table 4

**Analyzed Run Products from
Samples 17-22**

Copper-iron sulfides

Run #	Element in Atom %					Total %	Atom
	Ag	S	Au	Cu	Fe		
Run '17	0.0406	38.7651	0.045	53.2384	7.9109	100	
	0.0568	38.7496	0.0029	53.2872	7.9035	100	
	0.0541	38.6983	0.052	53.0456	8.01501	100	
Run '19	0.0361	38.9628	0.032	52.939	8.03	100	
	0.0617	39.818	0.0677	51.3082	8.7443	100	
	0.1928	39.8958	0.3015	50.4	9.2099	100	
	0.1361	39.9032	0.3133	50.9012	8.7463	100	
	0.1603	40.0049	0.2221	50.9558	8.657	100	
	0.1642	39.9404	0.0431	51.1368	8.7155	100	
	0.0853	39.8437	0.2002	51.2035	8.6673	100	
	0.0882	39.8863	0.3439	50.9633	8.7183	100	
	0.0714	39.9331	0.0706	51.306	8.6189	100	
	Run '20	0.5549	39.634	0.0112	51.1968	8.6031	100
0.5711		39.5728	0.0914	51.1047	8.6601	100	
0.2877		39.5944	0	51.4546	8.6633	100	
0.2964		39.4676	0.0147	51.5845	8.6369	100	
0.319		39.7448	0.1291	51.2746	8.5324	100	
0.3034		39.8078	0	51.3613	8.5274	100	
0.3537		38.9384	0.2453	51.7958	8.6668	100	
Run '21	0.0644	39.6491	0.0195	51.5287	8.7383	100	
	0.0575	39.9974	0.2986	51.0249	8.6216	100	
	0.0497	39.81	0.2167	51.2456	8.678	100	
	0.0371	40.0107	0.1709	51.1853	8.5961	100	
	0.0519	39.8009	0.1808	51.2815	8.6849	100	
	0.0469	39.8776	0.0332	51.3939	8.6484	100	
	0.0398	39.938	0.0113	51.3051	8.7058	100	
Run '22	0.0649	39.8334	0.1968	51.3619	8.543	100	
	0.1187	39.7715	0.0816	51.5969	8.4944	100	
	0.1503	39.5484	0.0263	51.7485	8.5265	100	
	0.1743	39.7198	0.0342	51.5243	8.5474	100	
	0.1236	39.6383	0.0467	51.6707	8.5207	100	
	0.1018	39.7324	0.058	51.7109	8.3969	100	
	0.0796	39.6146	0.0629	51.8076	8.4353	100	

1 % (1 σ) –see discussion of microprobe

From the successful runs log K values were derived based on the equilibrium constants:

$$K = \frac{x_{\text{Ag}}^{\text{sulfide}} * x_{\text{Cu}}^{\text{metal}}}{x_{\text{Cu}}^{\text{sulfide}} * x_{\text{Ag}}^{\text{metal}}}$$

for copper-silver exchange

$$K = \frac{x_{\text{Ag}}^{\text{sulfide}} * x_{\text{Au}}^{\text{metal}}}{x_{\text{Au}}^{\text{sulfide}} * x_{\text{Ag}}^{\text{metal}}}$$

for silver-gold.

Table 5

K values Cu-Ag	Log K Cu-Ag	K values Ag-Au	Log K Ag-Au
0.0198	-1.70	1218	3.09
0.0165	-1.78	20291	4.31
0.0115	-1.94	1255	3.10
0.0087	-2.06	1597	3.20
0.0617	-1.21	2420	3.38
0.1928	-0.71	2353	3.37
0.1361	-0.87	377	2.58
0.1603	-0.80	1050	3.02
0.1642	-0.78	3258	3.51
0.0853	-1.07	480	2.68
1.47	0.17	561837	5.75
0.348	-0.46	12875	4.11
0.190	-0.72	55890	4.75
0.137	-0.86	1977	3.30
0.012	-1.93	2101	3.32
0.011	-1.95	176	2.25
0.013	-1.90	316	2.50
0.012	-1.94	373	2.57
0.030	-1.52	1065	3.03
0.026	-1.59	4924	3.70
0.010	-2.01	143	2.16
0.019	-1.71	745	2.90
0.023	-1.64	2565	3.41
0.026	-1.59	2025	3.31
0.020	-1.71	1453	3.16
0.017	-1.76	1217	3.09
0.012	-1.92	681	2.83
$\mu =$ 0.122;	-1.36;	25358;	3.27
$\sigma =$ 0.274;	0.585;	107788;	0.763

V. Discussion of Results:

My dry sulfide experiments were conducted using the guidelines provided by Simon, et al (1998), for dry sulfide experimentation at 600°C and atmospheric pressure. My results were consistent with theirs; a change in concentration of gold from 0 ppm to 2986 ppm in the sulfide phases analyzed. Additionally, the gold foil demonstrated a change in silver concentration from 0 ppm to 2300 ppm and from 0 ppm to 5549 in the copper sulfide phases analyzed.

Upon examination under reflected light microscopy, there were some distinct crystal structures, perforated silver foil and weakly annealed masses. Under microprobe analysis there were distinct phase boundaries like the metal phase in Figure 4, silver-rich inclusions, un-reacted silver, copper-iron sulfide and electrum. Experiments 9-16, were conducted strictly to determine equilibrium, but there was no conclusive trend; increasing time (7-56 days) produced increasing ion exchange between the sulfide, silver and electrum phases with no discernible plateau. Complicating the results was the loss of electrum in some experiments during preparation for analysis. Simon, et al. (1998) discussed the same trend I observed: a range of gold concentrations from 0 ppm to >5000 ppm. For my purposes, a change in ppm was all that was necessary to establish that a reaction occurred.

To take my experiments from the dry environment of the laboratory to the wet hydrothermal system required a model for wet experimentation to which I could link my results. This was provided by Gammons, Williams-Jones (1995) research in solubility of Au-Ag alloy + AgCl in brine at 300°C. The temperatures used in the wet experiments correlate to the environment of a porphyry copper deposit and its associated epithermal deposit (see Figure 1). The higher temperature of my experiments is a consideration of the greater difficulty of ion transfer in the dry environment.

The final step is the experimental determination of the ore fluid that forms the epithermal body. All of my data have been presented in Atom percent, equivalent to moles, so I will continue to use moles

Taking the experimental determination of the concentrations of silver and gold from the laboratory to the mind based on the mean of my K values (LY): $K^{LY} = 25358 \pm 107788 (1\sigma)$ and the molar ratio of silver:gold at Far Southeast (FSE-L) epithermal deposit = 9.00 or $\text{Log } K^{FSE-L} = 0.95$ in the deposit. Multiplied together (with the understanding that each step enlarges the margin of error) yields 228287 or

$$\text{Log } K^{FSE-L} = 5.36.$$

For the hypothetical silver-gold concentration in the Far Southeast-Lepanto ore fluid that leaves the porphyry copper deposit to form the Lepanto ore body.

The Ag/Au ratio in the hypothetical median porphyry copper deposit (MPCD) is 15.00 or

$$\text{Log } K^{MPCD}_{(deposit)} = 1.18$$

so again, multiplying by my K^{LY} the experimental silver:gold concentration, the ore fluid leaving the median porphyry deposit becomes

$$\text{Log } K^{MPCD}_{(fluid)} = 5.58$$

At 600°C the temperature dependence factor (Equation 1) is 1.15 which translates to a log K value of approximately -3 which is consistent with the Gammons and Williams-Jones (1995) trend of increasing log K with increasing temperature. So the calculated fluid silver:gold ratio at 600°C is 0.001 normalized by

K^{LY} yields $\text{Log } K^{G\&W\text{-}J}$ of 1.40
and this becomes the metal ratio epithermal deposit.

VI. Conclusions:

Table 6 -Summary of Log K values

Log K Values	Ore	Fluid
$\text{Log } K^{LY}$	-----	4.40
$\text{Log } K^{FSE-L}$	0.95	0.36
$\text{Log } K^{MPCD}$	1.18	5.58
$\text{Log } K^{G\&W\text{-}J}$	-3.00	1.40

The calculated metal ratio in the epithermal deposit as determined by Gammon Williams-Jones (1995) is $\text{Log } K = -3.00$, and is significantly lower than the median epithermal deposit $\text{Log } K = 1.18$. Based on these results, the null hypothesis: **the partitioning of silver into copper-iron sulfides during the formation of a porphyry copper deposit will be insufficient to poison the formation of a shallow epithermal deposit**, was not supported.

These results are highly theoretical and for every mathematical operation conducted with actual and experimental results, the margin of error increases greatly. This mind experiment was simply an attempt to address the deficit in available data regarding ore deposits. Silver is present in the Earth's crust at a ratio of 43:1 with gold (Rudnick and Gao, 2003), and by virtue of that, if gold is present in sufficient quantities to form an epithermal deposit, silver should be present as well. Since the main constraint on ore metal ratios is the crustal abundances, the absence of an epithermal deposit points to a magma body depleted in ores or more likely, sequestering of ore metals by the process of mineralization. Research has shown that pyrrhotite and magnetite can sequester silver (Englander 2005) and bornite can accommodate up to 1 weight percent of gold (Simon, et al. 2000), so a median porphyry deposit like the one described in this paper could potentially reduce the epithermal budget by 20 tonnes for gold alone.

VII. Acknowledgements:

I would like to thank first and foremost my family and friends, all of whom have been very tolerant (though at times not very helpful) in my pursuit of this degree. I would like to thank my advisors, “the Phils” for working with me during the evolution of this project. And finally, the faculty and staff at Maryland for your contributions in shaping my educational experience.

BIBLIOGRAPHY

- Andesites. 2006. Geochemical Earth Reference Model: Reservoir Database. Ed. William McDonough. <Online<<http://earthref.org/GERM/index.html>>
- Ballantyne, G.H. 1997. Distribution and mineralogy of gold and silver in the Bingham Canyon porphyry copper deposit, UTAH. *SOCIETY OF ECONOMIC GEOLOGISTS* **29**,147-153.
- Barton, Jr., P. B.1970. Sulfide Petrology. *In Mineralogical Society of America special papers*. Mineralogical Society of America. **3** 187-198.
- Brooks, W.E. 2006 Silver. *In Mineral Commodity Summaries*. Online<<http://www.usgs.gov/minerals/pubs/mcs/2006>>
- Candela, P.A. 2004. The Crust: Ores in the Earth's Crust. *Treatise on Geochemistry*. Ed. Rudnick, R.L. **3**, Elsevier, Ltd 411-430 2004.
- Candela, P.A. 1997. A review of shallow, ore-related granites; textures, volatiles, and ore metals. *In* Seltmann, R., Lehmann, B., Lowenstern, J.B., *High level silicic magmatism and related hydrothermal systems; IAVCEI '97 selected papers*. *J PETROLOGY* **38**, 1619-1633.
- Candela, P.A. 1992. Controls on ore metal ratios in granite-related ore systems: an experimental and computational approach. *ROYAL SOC EDINBURGH: EARTH SCI.* **83**, 317-326.
- Candela, P.A, Piccoli, P.M., 1995. Model ore-metal partitioning from melts into vapor and vapor/melt mixtures. In: *Magma, Fluids, and Ore deposits*, Ed:Thompson, J.F.H., Mineralogical Association of Canada, 23, 101-127.
- Englander, L. I. 2005. AN EXPERIMENTAL STUDY OF SILVER PARTITIONING IN SULFIDE-OXIDE-MELT SYSTEMS AT 800° C. M.S. Thesis, University of Maryland,College Park: 144 pp.
- Donovan, J.J. ND. Electron Probe Microanalysis(EPMA): An overview (portions from J. I. Goldstein, D. E. Newbury, P. Echlin, D. C. Joy, C. Fiori, E. Lifshin, "Scanning ElectronMicroscopy and X-Ray Microanalysis", 2nd Ed., Plenum, New York, 1992). http://darkwing.uoregon.edu/~epmalab/UCB_EPMA/download/115EPMA.pdf.
- Gammons, C.H., & William-Jones, A.E. 1995. The solubility of Au-Ag + AgCl in HCl/ NaCl solutions at 300°C: New data on the stability of Au (I) chloride complexes in hydrothermal fluids. *Geochemica et Cosmochimica Acta.* **59** pp3453-3468.
- Halter, W.E., Pettke, T., Heinrich, C.A. 2002. The origin of Cu/Au ratios in porphyry-type ore deposits. *SCIENCE* **296**, 1884-1887.
- Harris, A. C., and Golding, S.D. 2002 New evidence of magmatic-fluid-related phyllic alteration: Implications for the genesis of porphyry Cu deposits. *GEOLOGY*: **30**, 335–338.
- Hedenquist, J.W., Arribas, Jr., A., Reynolds, T.J., 1998. Evolution of an Intrusion-Centered Hydrothermal System: Far Southeast-Lepanto Porphyry and Epithermal Cu-Au Deposits, Philippines. *ECONOMIC GEOLOGY AND THE BULLETIN OF THE SOCIETY OF ECONOMIC GEOLOGISTS.* **93.4**, 373-404.
- Hedenquist, J.W., Lowenstern, J.B. 1994. The role of magmas in the formation of hydrothermal ore deposits. *NATURE* **370**, 519-528.

- Heinrich, C.A., Driesner, T., Stefansson, A., and Seward, T.M., 2004. Magmatic vapor contraction and the transport of gold from the porphyry environment to epithermal ore deposits. *GEOLOGY*. **32.9**, 761-64.
- Jugo, P.J., Candela, P.A., Piccoli, P.M. 1999. Magmatic sulfides and Au:Cu ratios in porphyry deposits: an experimental study of copper and gold partitioning at 850°C, 100MPa in a haplogranitic melt-pyrrhotite-intermediate solid solution-gold metal assemblage, at gas saturation. Elsevier. *Lithos* 46. 573-589.
- Kullerud, G. 1971. Experimental Techniques in Dry Sulfide Research. Research Techniques for High Temperature and High Pressure. Ed. G.C. Ulmer. New York. 1971.
- Lovering, S. T. 1968. "Future metal supplies, the problem of capability [summ.]." *Oklahoma Geology Notes* **28.1**.
- McKinstry, H., 1959. Mineral Assemblages in Sulfide Ores: The System Cu-Fe-S-O. *ECONOMIC GEOLOGY AND THE BULLETIN OF THE SOCIETY OF ECONOMIC GEOLOGISTS*. **54**, 975-1001.
- Plumlee, G.S., 1998. Geoenvironmental Characteristics of Epithermal and Porphyry Deposits in Metallogeny of Volcanic Arcs. B.C. Geological Survey, Short Course Notes, Open File 1998-8, Section P.
- Robb, L. 2005. Introduction to Ore Forming Processes. Oxford, UK. Blackwell Publishing.
- Rowins, S.M. 2000. Reduced porphyry copper-gold deposits: A new variation on an old theme. *GEOLOGY*. **28**, 491.
- Rudnick, R.L., Gao, S., 2003. The Crust, In: *Treatise on Geochemistry*. Elsevier Publishing, 2003, Volume 3, pgs. 659.
- Sillitoe, R.H., Bonham, Jr., H.F., 1984. Volcanic Landforms and Ore Deposits. *ECONOMIC GEOLOGY*. **79**, 1286-98.
- Simon, G., Kesler, S.E., Essene, E.J., Chryssoulis, S.L., 2000. Gold in porphyry copper deposits; experimental determination of the distribution of gold in the Cu-Fe-S system at 400 degrees to 700 degrees C. *ECONOMIC GEOLOGY AND THE BULLETIN OF THE SOCIETY OF ECONOMIC GEOLOGISTS*. **95.2**, 259-70.
- Solomon, M., 1990. Subduction, arc reversal, and the origin of porphyry copper-gold deposits in island arcs. *GEOLOGY*. **18**, 630-3.
- Ulrich, T., Dunther, D., & Heinrich, C.A. 1999. Gold concentrations of magmatic brines and the metal budget of porphyry copper deposits. *NATURE*. **399**, 676-8.
- Williams, T.J., Candela, P.A., Piccoli, P.M., 1995. The partitioning of copper between silicate melts and two-phase aqueous fluids: An experimental investigation at 1kbar, 800°C and 0.5 kbar, 850°C. *CONTRIB. MINERAL PETROL*. **121**, 388-99.